Engineering Structures 207 (2020) 110192

Contents lists available at ScienceDirect

Engineering Structures

journal homepage: www.elsevier.com/locate/engstruct

Development of a new design approach of reinforced concrete structures based on strength reduction method

Oumaima Abra[a,b], Mahdi Ben Ftima[a,*]

[a] Department of Civil, Geological and Mining Engineering, Polytechnique Montréal, Montreal University Campus, P.O. Box 6079, Station CV, Montréal, Québec H3C 3A7, Canada

[b] IDAE s.e.n.c, 204 Saint Sacrement Street, Montreal, Québec H2Y 1W8, Canada

ARTICLE INFO

Keywords:
Reinforced concrete
Design
Strength reduction method
Strut-and-tie method
Nonlinear finite element
Explicit approach

ABSTRACT

The design of complex reinforced concrete structures or elements of structures can be a challenging task for practitioner structural engineers in some specific non-conventional projects. For these specific cases, the use of well-established and standard design methods such as sectional methods or strut-and-tie methods can result into complex and sometimes inappropriate designs. On the other hand, the use of sophisticated numerical methods such as nonlinear finite element methods is not common in these situations because of their complexity and the lack of consensus on their validity within the engineering community.

This work presents an innovative new design approach for complex reinforced concrete structures. The approach is inspired from the strength reduction numerical method, well-established in the field of slope stability in geotechnical engineering. It can be considered as an intermediate approach between the conservative and universally well accepted strut-and-tie method, and the powerful nonlinear finite element method. A new simple constitutive law for concrete has been developed for that purpose as a user subroutine under the software ABAQUS-Explicit. It allows for the degradation of concrete by gradually reducing its tensile strength during the analysis. This law is presented within an overall new framework for the design of reinforced concrete structure based on two steps. The structure is loaded in a first linear elastic step and then degradation of the tensile post-pic occurs in a second nonlinear step. At the end of this second step, a re-organisation of the internal stresses occurs within the structure. A resisting pattern and failure modes similar to those in the strut and tie models occur as well. Two application examples are presented at the end of the study and demonstrate the potential and the feasibility of the new approach.

1. Introduction

The design of reinforced concrete structures is a well-established field in the civil engineering practice. For conventional structures/elements of structures, the predictive equations of the codes can generally be used to design the geometry of concrete and to detail adequate reinforcement to withstand sectional forces already computed by a structural analysis, generally a linear elastic one. The sectional design method based on beam theory can be used to design flexural and shear reinforcement in the so-called B-regions where the Bernoulli's principle remains valid (Fig. 1a & b). However, this method fails in the regions where loading and boundary conditions are applied or near a change of geometry. Those disturbed regions, also called D-regions due to a nonlinear strain distribution as shown in Fig. 1c, are designed using more advanced methods. The strut and tie method, or S&T method, presented by Schlaich et al. [15] is widely used to design D-regions. It is based on the truss analogy where compression is taken by concrete struts and tension by reinforcement ties. The nodal zones are defined as the intersection between struts and ties (Fig. 1d). This method falls into the plastic design philosophy as a lower bound static method where only strength and equilibrium are satisfied. It therefore provides a conservative design for the D-regions when well used. However, the more complex the structure, the more difficult it becomes to develop S&T models. Furthermore, these models can lead to bad designs whenever the chosen load resisting path is too far from the real resisting path stemming from compatibility, which can be assessed only by using nonlinear finite elements. Fig. 2 shows an example of complex design in reinforced concrete. It is a special corner of the generator pits wall in powerhouse hydraulic structure which transfers a horizontal force F. Fig. 2a presents the linear finite element (FE) model that helped to

* Corresponding author.
E-mail addresses: oumaima.abra@polymtl.ca (O. Abra), mahdi.ben-ftima@polymtl.ca (M. Ben Ftima).

https://doi.org/10.1016/j.engstruct.2020.110192
Received 13 March 2019; Received in revised form 22 July 2019; Accepted 8 January 2020

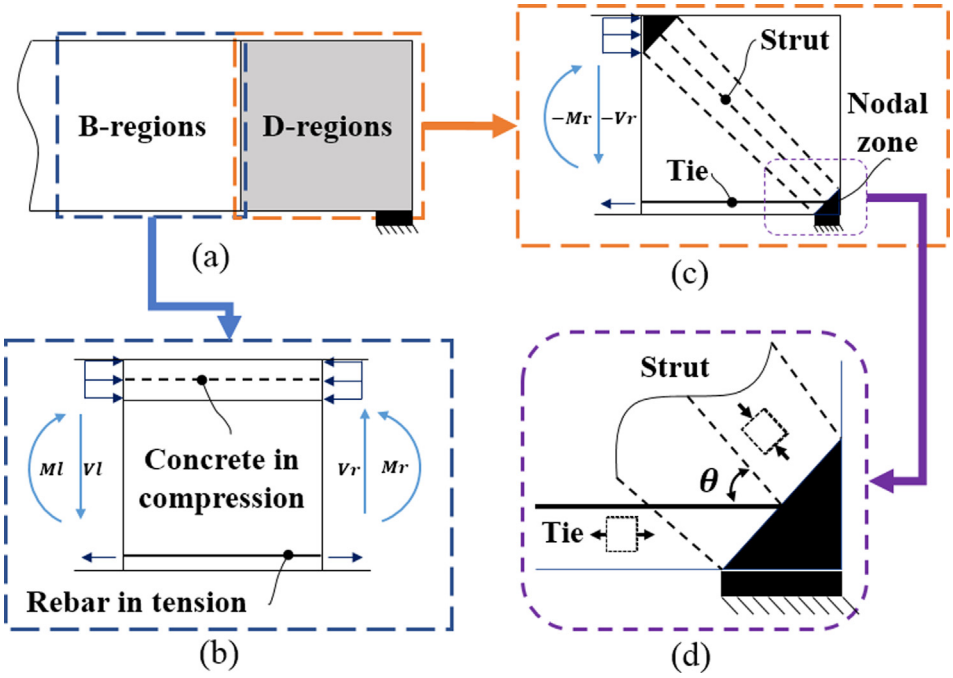

Fig. 1. (a) Example of the definition of B and D regions and distribution of the internal stresses in (b) B region and (c) in D region with (d) Zoom into the nodal zone.

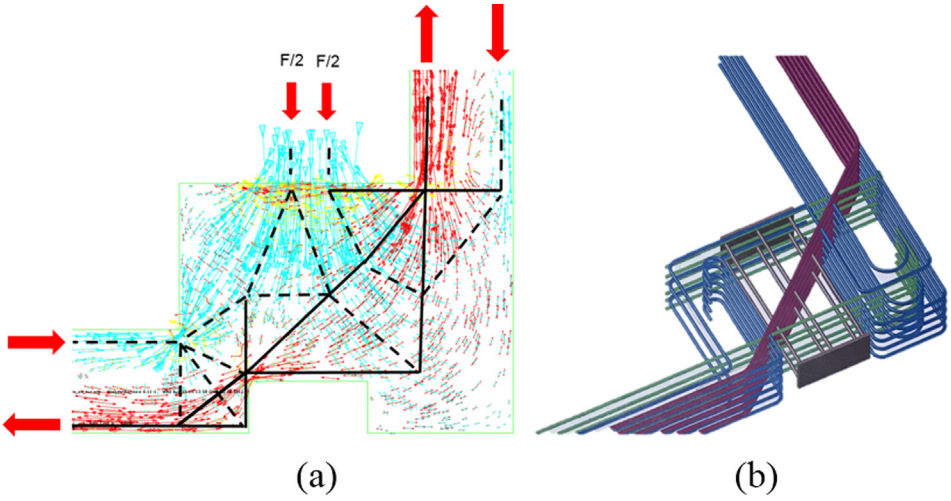

Fig. 2. Example of a complex reinforced concrete design: (a) extraction of a strut and tie model using linear FE analysis and (b) final reinforcement layout.

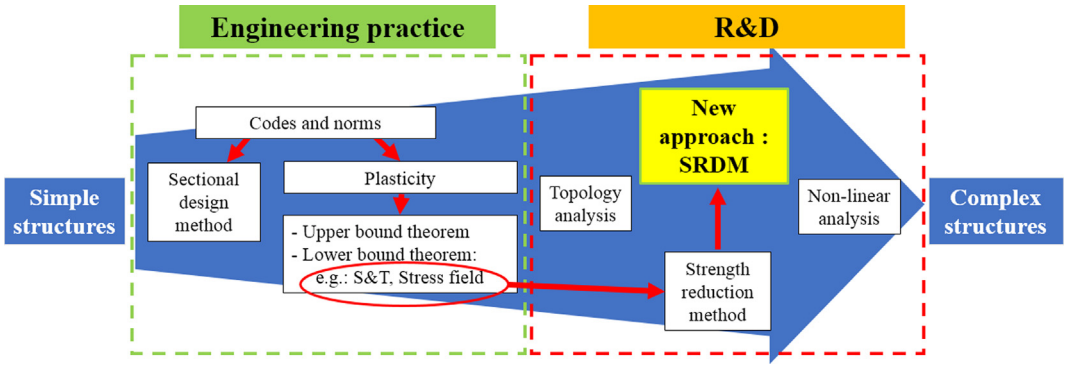

Fig. 3. Towards a new design philosophy.

develop the S&T method. Many iterations were required before reaching the final rebar layout shown in Fig. 2b.

Sophisticated tools as non-linear FE can be used to solve these complex design problems but are generally reserved to the R&D field and not commonly used in engineering practice.

The scope of this work is the development of an automatic/semi-automatic new design method suitable for complex reinforced concrete structures. The approach is inspired from the strength reduction numerical method and can be considered as an intermediate approach between the conservative and universally well accepted strut-and-tie method, and the powerful nonlinear finite elements method.

The paper is organised as follows. First, a critical literature review is presented in Section 2, in order to introduce the new design philosophy. Section 3 presents the computational framework developed for the set up of the new design philosophy. Preliminary verifications are presented in Section 4. Finally, in Section 5, two application examples are considered to illustrate the performance of the proposed approach.

2. Towards a new design philosophy

Fig. 3 summarizes the current state of the art concerning the design methods for reinforced concrete structures.

2.1. Engineering practice – conventional RC structures

In the engineering practice, the sectional design and the S&T methods are the most used methods, respectively for the B and D-region. Since it is based on the lower bound plasticity theorem, the S&T is still applicable in the B-regions. The upper bound and lower bound plasticity theorems were formulated by [5]. They are considered as extremum principles for rigid plastic materials [11]. Methods based on upper bound plasticity theorem (e.g. yield line method for slabs- [8] provide simple ways to design conventional concrete elements, even though they are always unsafe from the theoretical point of view. The design methods based on the lower bound solution are most interesting since they 'theoretically' are on the safe side. The lower bound theorem states that if the load has such a magnitude that is possible to find a stress distribution within the admissible strength of the materials (concrete and reinforcement) and satisfying the equilibrium and boundary conditions (i.e. statically admissible), then this load will not cause the collapse of the structure. The S&T method [15] and the stress field method [10] are examples of design methods issued from the lower bound theorem. Both S&T and stress field methods provide a phenomenological description of the post-cracking reinforced concrete behaviour, leading to simple models. The development of stress fields/S&T truss remains mainly based on intuition and experience. According to Schlaich et al. [15], the elastic stress field (e.g. from linear FEM) can be used to inspire the truss model and the minimum strain energy criterion can help single out the suitable model. Those guidelines allow the choice between different models but does not give guidance towards the real flow of stresses that can be very different from the elastic response. Also, this flow depends on the reinforcement layout and not just on the loading and the geometry. Several computer-based tools have been developed over the time to facilitate the use of the strut and tie method (e.g. [16]), but still their applicability is limited to simple models.

The limitations of plasticity-based design methods are linked to the rigid-plastic assumption which is a drastic simplification of the reality of RC structures. The most critical issue is the assumption of a certain ductility within the RC structure in order to reach the anticipated flow of stresses, but there is no guaranty that this flow is attainable. In fact, there is possibility of brittle failure mechanism (e.g. shear) or disturbance of stress flows due to the existence of pronounced discrete cracking (e.g. thermally induced stresses during construction). Design codes impose generally a minimum amount of reinforcement in order to allow for a minimum ductility to accommodate the discrepancies between the designed flow of stresses and the real one. Such minimum amount can result sometimes in non-economical designs or congestion of rebars and is unfeasible for the specific case of large and lightly large reinforced concrete structures (e.g. powerhouses, spillways…). Furthermore, it is difficult to use these methods to assess the effect of loads driven by deformation like the thermal loads, creep, shrinkage, problems due to settlement or problems due to concrete swelling (e.g. alkali-aggregate reaction).

2.2. R&D – complex RC structures

Topology optimization and non-linear finite elements have been developed during the past years as additional tools for designing complex RC structures or checking existing ones.

2.2.1. Topology optimization

Researches have been undertaken using topology optimization, a method that is largely used in the aerospace and mechanical industries where the purpose is to optimize the quantity of material. In structural engineering, topology optimization is used to find the optimal distribution of materials by neglecting the contribution of concrete in tension. Bendsoe and kikuchi [3] proposed the Homogenized based optimization or HBO, based on the redistribution of material properties and homogenization theory. Other methods have been developed since then. To monitor the optimization process, Liang et al. [9] developed the performance index PI that allows to generate a truss like structure. The most popular method for reinforced concrete structures is the evolutionary structural optimization (ESO) presented by Xie and Steven [20], based on a progressive material removal criterion using finite elements. Many methods evolved from the ESO such as the Bidirectional Evolutionary Structural Optimization or BESO method by Querin and al. [13].

One of the major problems concerning the topology optimization methods is the difficulty to take into consideration the specific aspects related to construction of RC structures: difficulty to place inclined reinforcement layers or construct complex geometries of concrete elements. Constructibility issues have been partially considered in Bairan [1] where the author used topology optimization combined to linear elastic analyses to produce Strut and Tie models, while using a specific constraint for the condition of orthogonal reinforcement.

Considering the current state of the art in topology optimization, it can be said that these methods can be used to produce optimal strut and tie models and are not suitable for a direct use as design methods. More specifically, none of these method does allow for the strength assessment of struts and nodal zones.

2.2.2. Non-linear finite element

Non-linear finite element using validated constitutive model for concrete is considered as the only tool capable of predicting the *true* path of flows in post-cracked RC structures, by fulfilling requirements of both lower bound and upper bound plasticity theorems: equilibrium, strength and kinematically admissible displacement field. This sophisticated tool is generally reserved to the R&D field or to the assessment of existing critical RC structures. It is not commonly used in the engineering design practice, mainly due to four facts: (i) the lack of consensus on a universal constitutive law for concrete; (ii) the complexity of the analyses and the difficulty to assess the required input parameters; (iii) the need to start from an initial design (geometry of concrete element and layout of rebars) and to perform iterations using different configurations in case of detected failure in the non-linear FE model and (iv) due to the contribution of concrete in tension (not negligible in case of large members), it is difficult to assess with this method the real demand on the reinforcement, especially for the case of statically indeterminate structures.

To overcome the problem of tensile contribution of concrete, it is still possible to use non-linear finite element but with very low values of

the tensile strength. Ruiz and Muttoni [14] presented an approach towards the automatic development of stress field based on nonlinear finite element method. The constitutive model is relatively simple and requires a limited number of input parameters: compressive strength and modulus of elasticity. The tensile strength is neglected.

The main problem with this approach is the consideration of a loading pattern on a virtually 'already cracked' structure which may not be representative of the real behaviour of RC structures and may influence the flow of stresses. Also, similarly to S&T and stress field methods, it is difficult with this kind of approaches to assess the effects induced by deformation such as thermal effects.

2.2.3. Strength reduction

The strength reduction is a method used in the geotechnical engineering field for quantifying slope stability. It was first presented by Zienkiewicz et al. [21] and is based on the gradual decrease of the resistive strength of materials along potential plans of weakness. It was applied by many researchers to compute the factor of safety and locate the critical slip surface (e.g. [17]). More recently in [19], this method was used to evaluate sliding stability of hydraulic structure 3D concrete blocks using the quasi-static explicit nonlinear finite element (QSE-FEM) approach known for its efficiency in solving highly non-linear problems compared to implicit FEM.

2.3. Development of new design approach

The philosophy behind the strength reduction approach is very interesting and constitutes the first main motivation behind this work. The idea is to apply the load on the structure by using a simple linear constitutive model and then apply a progressive reduction of the tensile strength to allow the redistribution of stresses between the reinforcement in tension and the concrete in compression.

The second main motivation behind this work is the worldwide consensus, within engineering and scientific communities, on the fact that the S&T method provides designs which are on the conservative side. So, rather than developing or using a sophisticated non-linear constitutive law (e.g. plasticity, damage theory, …etc.), the idea is to develop a simple non-linear law inspired from the three possible failure mechanisms of a S&T model: failure of the strut, of the tie or of the nodal zone (Fig. 1d).

The new design method called the Strength Reduction Design Method (SRDM) can be therefore viewed as an intermediate approach between the conservative and universally well accepted strut-and-tie method, and the powerful nonlinear finite elements method (Fig. 3).

The developed approach offers three main advantages: (i) it is oriented towards the automatic/semi-automatic design of RC structures, the designer can start the analysis using any pattern of reinforcement; (ii) it fulfils equilibrium, compatibility and strength conditions: the departure is linear elastic state of stresses fulfilling only equilibrium and compatibility, the final state (if reachable) fulfils the three conditions. The process of strength reduction can be compared to a uniform degradation process that may occur for any existing RC structure; and (iii) it requires only four physical and easily measurable input parameters: the Young modulus of concrete, the Young modulus of steel reinforcement, the Poisson ratio of the concrete, the compressive strength of concrete and the yield strength of reinforcement. Knowing the available semi-empirical relations for concrete and steel, only *two main input parameters* are actually required: the compressive strength of the concrete and the yield strength of the reinforcement.

A flowchart of the proposed methodology is presented in Fig. 4. First, the structure is modelled by defining the geometry of concrete, the material properties, the loading and the boundary conditions (step 1). The steel reinforcement is placed inside the concrete with a given layout of longitudinal and transverse rebars (step 2). The layout may be chosen to facilitate the installation of the reinforcement beds during the construction process. Depending on the available computational

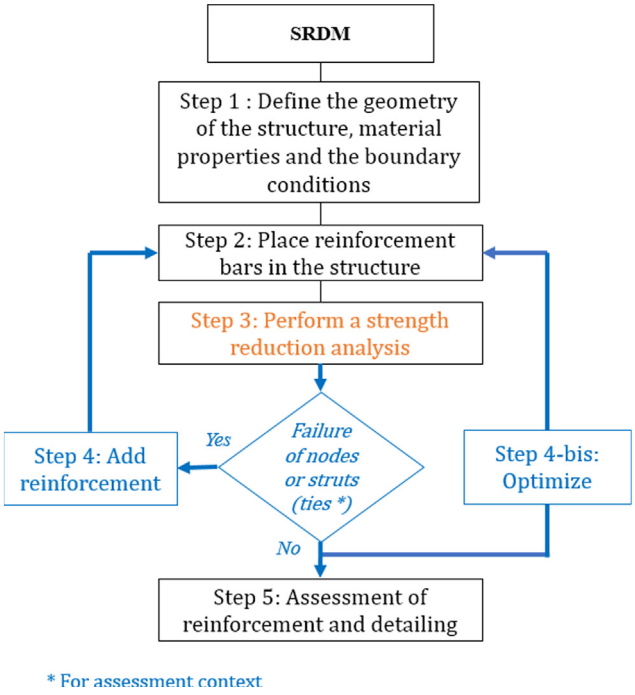

Fig. 4. Flowchart of the strength reduction design method.

framework, reinforcement may be modelled as 1-D truss elements embedded in 3D solid elements representative of concrete elements [7]. The strength reduction analysis is performed in the step 3 and includes two phases: a loading phase and a reduction phase. At the end of this analysis, failure of nodes, struts or ties may occur or not. At this level, the SRDM can be used in both new design and assessment contexts. For the assessment context, the failure of reinforcement ties (already known) may be activated by using a simple uni-axial plasticity law. In the context of a new design, which is the main context considered in this work, failure of the rebars is deactivated by using a linear elastic constitutive law. It is possible therefore to assess the demand on the reinforcement.

In case of failure (step 4), adjustment of the reinforcement layout is made by adding reinforcement (e.g. adding shear reinforcement in case of nodal failure).

In case of no failure (step 5 or 4-bis), it is possible to proceed whether to optimization of the reinforcement (step 4-bis) by removing some rebars, or to the final assessment, anchorage and detailing of the reinforcement (step 5).

Two main challenging numerical issues need to be solved for the correct implementation of the strength reduction analysis in step 3. The first one is the numerical difficulty in solving the non-linear problem during the strength reduction phase, the second one is the representation of failure of the nodal zone in the material constitutive law. Both issues are considered in the next section.

3. Computational framework

3.1. Quasi-static explicit analysis

The explicit dynamics approach was developed and successfully applied in the industrial field of metal forming at the beginning of the nineties in the industrial field of metal forming [12] and was implemented in several FE commercial packages as Abaqus [7] within the Abaqus-Explicit framework. Compared the implicit and iterative solver approach, the explicit solver is known for its efficiency in solving highly non-linear problems involving material softening [4].

Following an explicit formulation, the nonlinear problem is solved

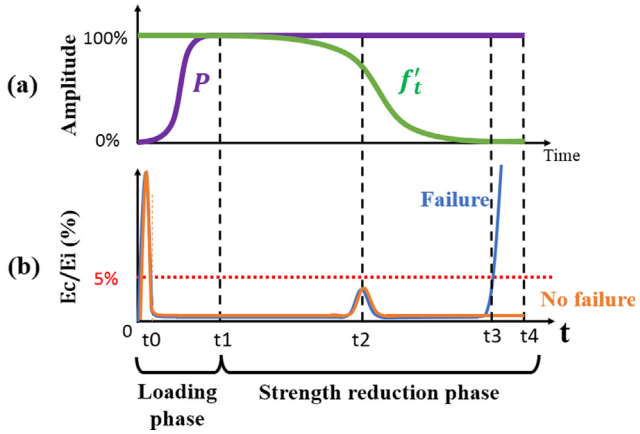

Fig. 5. Strength reduction analysis procedure: (a) Application of loads and reduction of strength; (b) Explicit analysis: Kinetic energy and internal energy ratio.

using dynamic equilibrium equations. Conventional nodal forces are converted into inertia forces by assigning lumped masses to nodal DOFs. The dynamic equilibrium equations are written in terms of inertia forces, where $\boldsymbol{M}$ is the lumped mass matrix of the model, $\boldsymbol{P}$ is the external load vector, $\boldsymbol{I}$ is the internal load vector and $\ddot{\boldsymbol{u}}$ is the nodal acceleration vector:

$$\boldsymbol{M\ddot{u}} = \boldsymbol{P} - \boldsymbol{I} \tag{1}$$

The explicit solver is used in this work but within the specific context of quasi-static finite element analysis QSE-FEM developed in previous works [4,19]. Hence the loads are applied *slowly enough* to minimize the kinetic over internal energy ratio of the system $\boldsymbol{E_c}/\boldsymbol{E_i}$. The rule of thumb established in previous studies is used in this work and consists on applying the loads using smooth steps and within a period of time equal to 20–40 times the fundamental period of vibration $\boldsymbol{T}$ of the structure. Fig. 5 shows an example of application of the load $\boldsymbol{P}$ following a smooth amplitude, using a 5th order polynomial function given in the following equation:

$$\boldsymbol{f}(\boldsymbol{x}) = \boldsymbol{x}^3 * (10 - 15 * \boldsymbol{x} + 6 * \boldsymbol{x}^2) \tag{2}$$

where x is the ratio between the analysis time $\boldsymbol{t}$ and the time at the end of loading phase step $\boldsymbol{t_1}$.

In this case, if $\boldsymbol{t_1}$ is chosen as 20–40 times $\boldsymbol{T}$, the kinetic over internal energy ratio will have the typical evolution depicted in Fig. 5 which can be considered quasi-static, despite the presence of the initial acceleration period from 0 to $\boldsymbol{t_0}$, necessary for the initial propagation of waves.

3.2. Loading and strength reduction phases

The proposed method is based on a QSE-FEM analysis with two phases (Fig. 5). In the first phase [0, t_1], the structure is gradually subjected to the loading or combination of loads. At this phase any reasonably high value of the tensile strength f_t' can be selected in order to maintain a linear elastic response of the model. In the second strength reduction phase [t_1, t_4] and while maintaining the previously applied loading (P remains constant after t_1) the tensile strength is gradually and isotopically reduced in all the structure to a very low negligible value. This degradation is done following a smooth step using a polynomial function similar to the one given in Eq. (2). It is performed incrementally following the stable increment time of the explicit solver and slowly enough to allow for a quasi-static redistribution of the stresses during the degradation phase. For the reduction phase to remain quasi-static when the tensile strength is reduced, the choice of a duration of the reduction phase ($t_4 - t_1$) three to five times as the duration of the loading phase (t_1) was found to be adequate in this study.

As depicted in Fig. 5, intermediate non-linear events may occur during the degradation phase, for example crack initiation and propagation at t2. For the degradation phase, two different situations may occur: (i) failure before the end on analysis (e.g. local failure in the nodal zone followed by collapse of the structure at t_3) which can be detected by an irreversible augmentation of the kinetic over internal energy ratio; (ii) no failure before the end of the strength degradation phase at time t_4, where the tensile strength reaches a value close to zero.

3.3. Constitutive law

Many constitutive laws have been developed over the last decades to simulate the complex behaviour of reinforced or un-reinforced concrete. By trying to recreate as many phenomena as possible, those models often require many input parameters very hard to define even with experimental tests. As the purpose here is not towards recreating the exact behaviour of concrete, a simple constitutive law has been developed, based on orthotropic elasticity and assuming the principal following hypotheses: (i) alignment between principal stresses and strain directions; (ii) strain rotating crack models; (iii) cracking is modelled using the smeared cracking approach [2] (iii) Once the cracking occurs in one principal direction, the model follows an orthotropic behaviour with respect to the cracking plane using an incremental stress/strain relationship and by ignoring Poisson's ratio effects (iv) Following the S&T hypothesis, the confinement effects are ignored.

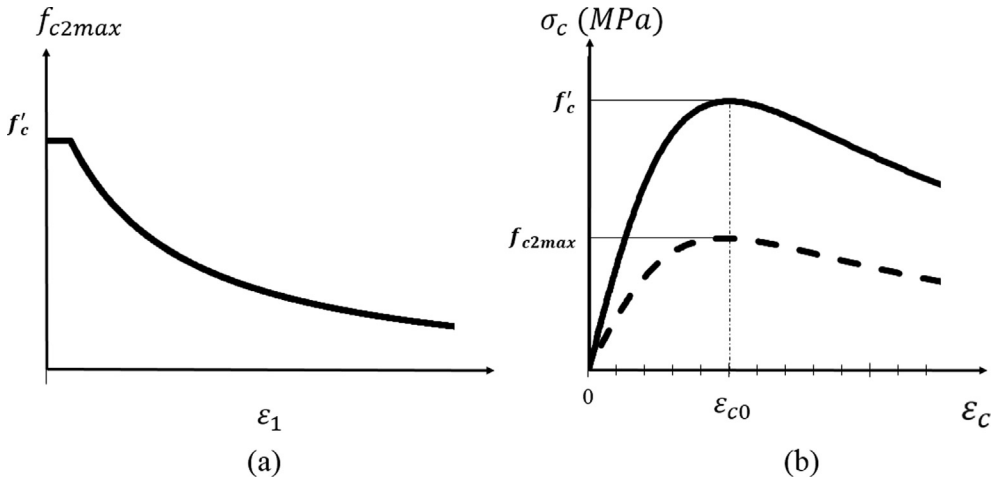

Fig. 6. Modified compression field theory and compressive response in concrete.

3.3.1. Uniaxial stress/strain law

For the compression case (Fig. 6), the Todeschini model (1964) is considered using the following stress/strain relationship:

$$\sigma_c = \frac{f_c^{'} * (\frac{\varepsilon}{\varepsilon_{c0}})}{1 + \left(\frac{\varepsilon}{\varepsilon_{c0}}\right)^2} \quad (3)$$

where ε_{c0} is the strain corresponding to the compressive peak taken as 0.002 in this study, given the known low variability of this parameter for normal strength concrete (from 0.002 to 0.0025).

Following the modified compression field theory (MCFT - [18], the original compressive strength is reduced from $f_c^{'}$ to $f_{c2max}$to take into account the effect of the principal transverse tensile strain ε_1 on the compressive strength of the strut. This ingredient is very important in the model since it is representative of local incompatibility in the S&T model, within the nodal zone when compressive and tensile forces meet (Fig. 1c).

The following relationship is used:

$$f_{c2max} = \frac{f_c^{'}}{0.8 + 170 * c * \varepsilon_1} \leq f_c^{'} \quad (4)$$

where c is an adjustment factor calibrated according to the S&T method and to achieve a certain mesh independency of the analyses as it will be shown in the next section (c = 1.0 in the original MCFT version of [18].

When the principal tensile stress reaches the peak in tension, concrete cracks and the residual strength decreases according to a post-cracking law. In this work, a simple linear stress-strain curve is used for the post-cracking behaviour as shown in Fig. 7, where ε_y is the reinforcement yield strain.

3.3.2. Reduction of tensile stresses

The strength reduction method is applied on the tensile strength of concrete $f_t^{'}$ according to the smooth law presented in Fig. 5. When the strength reduction phase begins, the global properties of concrete are modified, which affects the general tensile behaviour. The description of the reduction process is schematically presented in Fig. 7 by considering the example of a cantilever beam loaded by a force P and considering the two elements A and B within the mesh of the beam.

The strength reduction of the tensile stress/strain curve is schematically shown for three different states 0, I and II, respectively the blue, green and orange[1] curves. The state 0 denotes here the original state of the model at the end of the first loading phase (see Fig. 5). In the real analysis, the stress/strain curve is updated continuously at each explicit time increment ***ti*** by joining the peak stress point ($\frac{f_t^{'(ti)}}{E}$, $f_t^{'(ti)}$) and the zero stress point (ε_y,0). ε_y is yield strain of steel reinforcement with a typical value of 0.002. $f_t^{'(ti)}$ is obtained from the smoothly decreasing law of $f_t^{'}$ depicted in Fig. 5, corresponding to a given explicit time increment ***ti***. At the beginning of the strength reduction phase, the two elements A and B are at different stages $A^{(0)}$ and $B^{(0)}$ located on the original uniaxial curve (the blue-coloured curve). The point $A^{(0)}$ corresponding to the most stressed element in tension A, is located at the peak of the stress/strain law, because as said before, the initial tensile strength of the material ($f_t^{'(0)}$) is selected sufficiently high so that the analysis in the first phase remains linear elastic.

In state I of strength reduction phase, the tensile strength is decreased to $f_t^{'(I)}$ and as shown in Fig. 7, the element A follows a modified stress/strain curve. Element B on the other hand remains in the elastic part because it is not yet affected with the reduction of tensile strength: the stress level is less than the tensile strength $f_t^{'(I)}$ at the state I. In state II however, the tensile strength decreases considerably and, under the strain increment $d\varepsilon_B^{(II)}$, the element B goes into softening.

[1] For interpretation of color in Fig. 5 and 16, the reader is referred to the web version of this article.

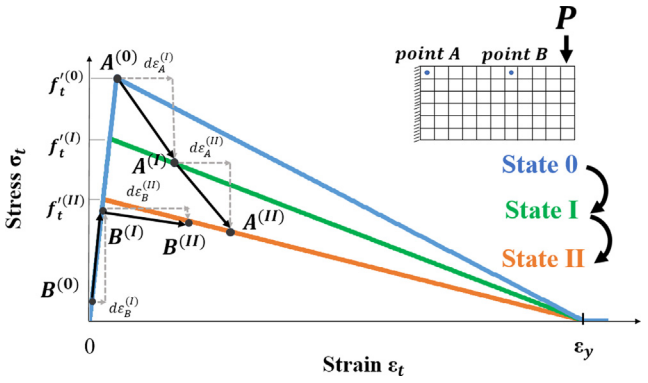

Fig. 7. Strength reduction method: effect on the uniaxial tensile stress and strain curve.

4. Verification and calibration

4.1. Biaxial behaviour under degradation

Series of numerical biaxial tests were performed on a single finite element as shown in Fig. 8 at three different values of the reduced tensile strength: 100%, 50% and 1%. Each point in each of the three envelopes represents a different non-linear analysis with a fixed $\frac{\sigma_3}{\sigma_1}$ ratio.

Each of the three envelopes can be assimilated to the yield surface within the plasticity constitutive framework but are actually failure surfaces for the orthotropic constitutive framework used in this work. The square shape of the failure surface for compression/compression is consistent with the hypothesis of ignoring the confining effects. Finally, as anticipated, the effect of the strength reduction on the biaxial behaviour of the element is validated. The evolution of the biaxial failure surface shown in Fig. 8, represents a typical behaviour of an element of the FE model during the strength reduction phase. This behaviour will allow the redistribution of the stresses between concrete compressive struts and tensile reinforcement ties.

4.2. Uni-axial behaviour of a reinforced concrete element

In order to verify the transfer of stresses between concrete and reinforcement during cracking, a simple 3D solid element with one integration point is loaded in tension as shown in Fig. 9.

The reinforcement is modelled using truss elements and is embedded in concrete. The SRDM is first used for this example in the assessment mode where a non-linear constitutive uni-axial law is used for the rebar element with a yield strength f_y = 400 MPa. The applied force ***P*** at the loading phase is set equal to ***As. f_y***, where ***As*** is the cross section of the rebar. As shown in Fig. 9, at the beginning of the strength reduction phase, the rebar is not fully working since concrete is still able to carry some tensile stresses. This situation can happen in the case of a non-linear finite element model as stated in Section 2 and constitutes a limitation for this category of analyses for the specific purpose of designing RC structures. The advantage of the SRDM is clear here, since as concrete is losing strength, the stress in rebar increases gradually until reaching the yield strength.

The same example can be used in design mode (dotted line in Fig. 9). In this case, a linear constitutive law is used for reinforcement. The behaviour of reinforcement is linear elastic throughout the analysis. The final stress $\sigma_s$developed in the rebar after the end of the strength reduction phase (if possible, without failure of struts or ties) allows to compute the required reinforcement using the following equation:

$$A_{s,required} = A_{s,initial} \times \frac{\sigma_s}{f_y} \quad (5)$$

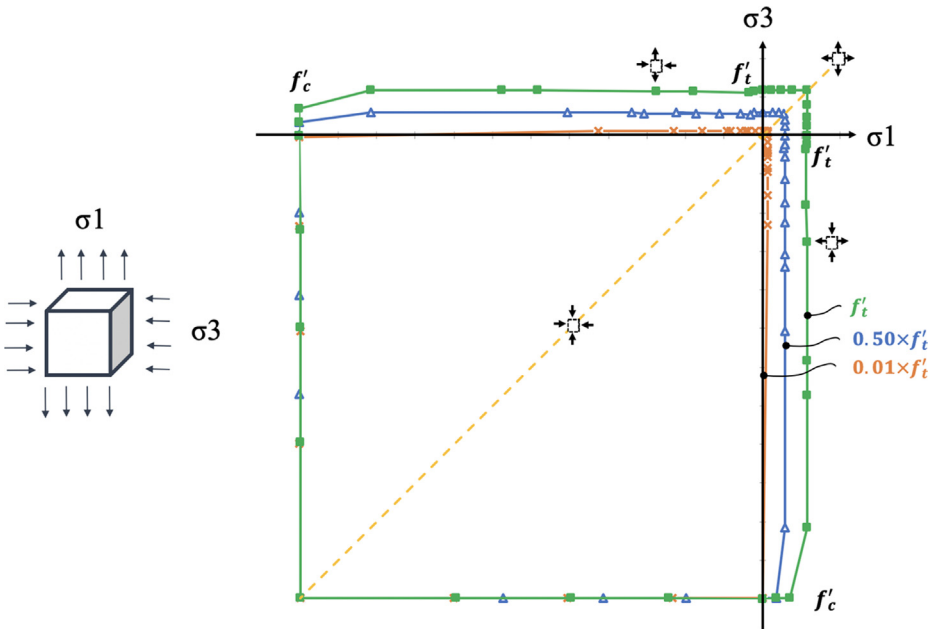

Fig. 8. The effect of the strength reduction of the tensile strength of concrete on the biaxial failure surface.

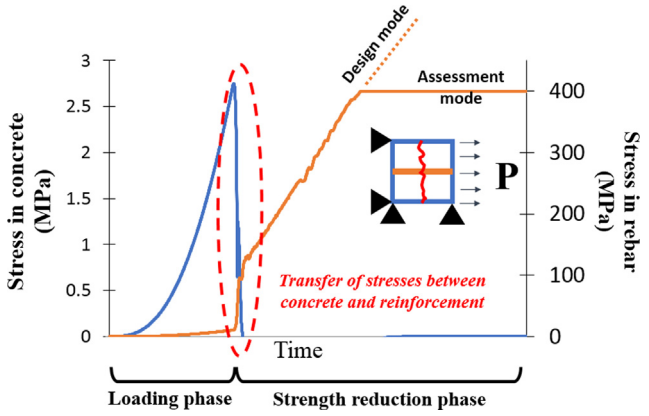

Fig. 9. Behaviour of a reinforced concrete element: before and after cracking of concrete.

4.3. Calibration

The modified compression field theory (Eq. (4)) presented before, translates the incompatibility at the nodal zone where the tensile strain in the ties and the compressive strain in the strut meet. If the strut is very inclined compared to the ties, incompatibility of strains occurs, and the failure of the nodal zone happens. Within the FEM framework, this failure occurs by local crushing of concrete elements close to the nodal zone, when the principal compressive stress σ_{min} reaches the the compressive strength (f_{c2max})reduced by the effect of transverse tensile strains (Fig. 10d). It is possible therefore to define a parameter β monitoring the ratio between the principal compressive stress σ_{min} and the reduced compressive strength f_{c2max}:

$$\boldsymbol{\beta} = \frac{\boldsymbol{\sigma_{min}}}{\boldsymbol{f_{c2max}}} \tag{6}$$

The direct use of the original MCFT (Eq. (4) with $\boldsymbol{c}$ = 1 0.0) in the context of SRDM using FEM raises two problems: (i) The Eq. (4) has been developed in an average sense at the level of a RC panel and not at the local level of an element within the mesh of nodal area; (ii) The direct use of a strain in the denominator raises the problem of mesh dependency known in the literature for this method.

The adjustment factor $\boldsymbol{c}$ is introduced in this work to address these problems. For the SRDM to be quasi mesh independent, a crack width rather than a strain must be used in the denominator and therefore the adjustment factor $\boldsymbol{c}$ is chosen proportional to the nominal dimension $\boldsymbol{h}$ of the mesh used in the model. To simplify the discussions, the mesh is assumed cubic with a uniform edge length $\boldsymbol{h}$.

To address the first problem, the S&T method is used to calibrate the $\boldsymbol{c}$ factor using a geometry of a RC cantilever beam (Fig. 10a). The cantilever configuration can be viewed as the simplest RC element representing the three components of a S&T model: the tie (horizontal), the strut (inclined) and the nodal zone at the tip of the beam where the load $\boldsymbol{P}$ is applied. Fig. 10b presents three configurations of the nodal zone with three different inclinations of the strut: from $\theta = 25^{\circ}$ for the short cantilever beam to $\theta = 13^{\circ}$ for the long cantilever. A limit cantilever geometry is chosen to a limit value $\theta = 20^{\circ}$ chosen for the inclination of the strut. It can be seen that for values of θ less than 20°, the strength of the concrete near the strut/node area can be reduced down to 15% of the initial compressive strength of concrete (for usual value of 0.002 of ε_s and ε_2 in Fig. 10d), therefore, the size of the nodal area becomes excessively large as shown in Fig. 10b.

For the limit cantilever geometry, and for different mesh sizes, series of FEM simulations have been performed in order to find the limit value of $\boldsymbol{c}$ for which the parameter β approaches the limit value of 1.0 near the nodal zone as shown in Fig. 10c.

Using the described methodology, it is possible to plot the limit value of the parameter $\boldsymbol{c}$ for different mesh sizes as shown in Fig. 11a.

A linear equation is used to represent this dependency and is given by the following equation:

$$\boldsymbol{c} = 1.187\frac{\boldsymbol{h}}{1000\ \ \mathbf{mm}} + 0.083 \tag{7}$$

where $\boldsymbol{h}$ is the nominal size in mm of an element of the mesh used.

With the use of Eq. (7) along with Eq. (4) given before, the limit compressive stress f_{c2max} is represented in Fig. 11b for different mesh sizes and is compared to the original MCFT law (with $\boldsymbol{c}$ = 1.0).

The parameter β is an important parameter in the SRDM and can be used to monitor the analysis during the strength reduction phase. Higher values of β (more than 0.9) towards the end of the analysis are generally signs of potential problems in the nodal zones. When the limit value of 1.0 is reached, the nodal zone fails with a crushing failure type equivalent to sliding along a plane as it will be shown later. This

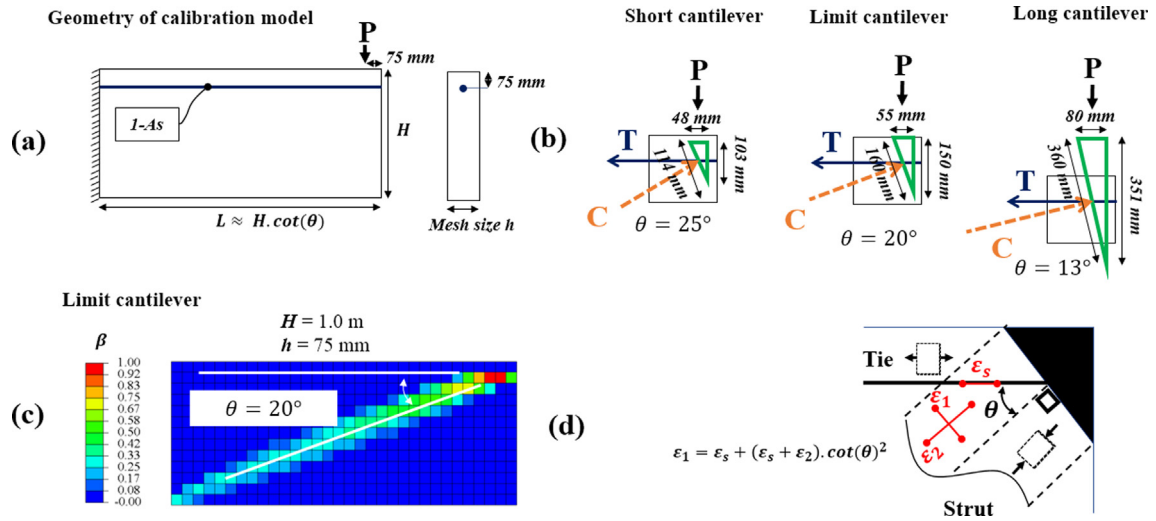

Fig. 10. Calibration model for the adjustment factor *c*: (a) Geometry of the cantilever model, (b) Nodal zone geometry at the end of the beam; (c) Example of FEM model with limit geometry and (d) Idealization of the nodal zone.

generally corresponds to the failure of the model with an irreversible increase of the kinetic over internal energy ratio (Fig. 5). In this case, the design is inadequate and additional ties must be added to the model (Fig. 4 – step 4) to adjust the inclination of the struts.

5. Applications

To evaluate the performance of the developed SRDM, two application examples are presented in this section. The first application considers the simple geometry of cantilever RC beam with different configurations. In the second application, a study of a statically indeterminate beam with an opening considered in previous works is presented.

5.1. RC cantilever beam

Three different cantilever beams are considered in this application (Fig. 12). A short cantilever beam CB1 and two long cantilever beams CB2 and CB3. The out of plane dimension of the beams is 500 mm.

For each configuration, the load P was computed to ensure a stress value of 400 MPa for the rebars at the critical section of the cantilever using the sectional design method. Hence, the stress on reinforcement shall converge to this value at the end of the strength reduction phase, if attainable without failure in concrete (within struts or nodal zones).

Fig. 13 shows the results obtained for the short cantilever beam CB1. At the end of the strength reduction phase, the configuration of the principal compressive stresses shown in Fig. 13a, recalls the layout of an inclined strut in the S&T model. A zoom into the end of the beam where load is applied, shows a flow of compressive stresses which also recalls the case of a CCT node in the S&T model. Fig. 13b shows the

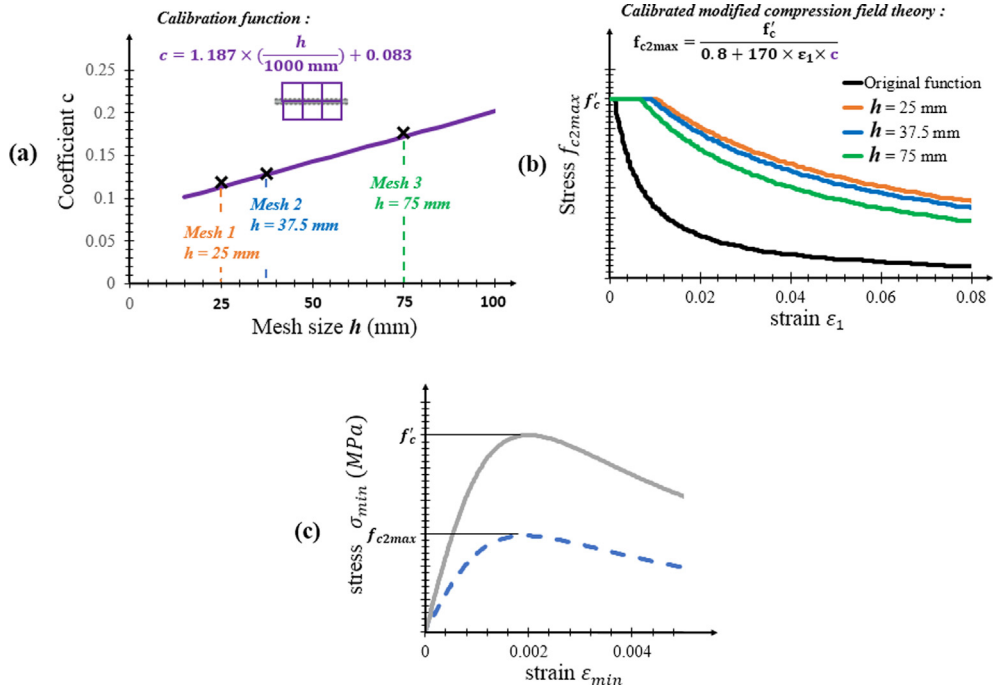

Fig. 11. Calibration of the parameter *c* for MCFT: (a) Dependency on the mesh size (b) Calibrated MCFT; (c) Stress-strain curve in compression.

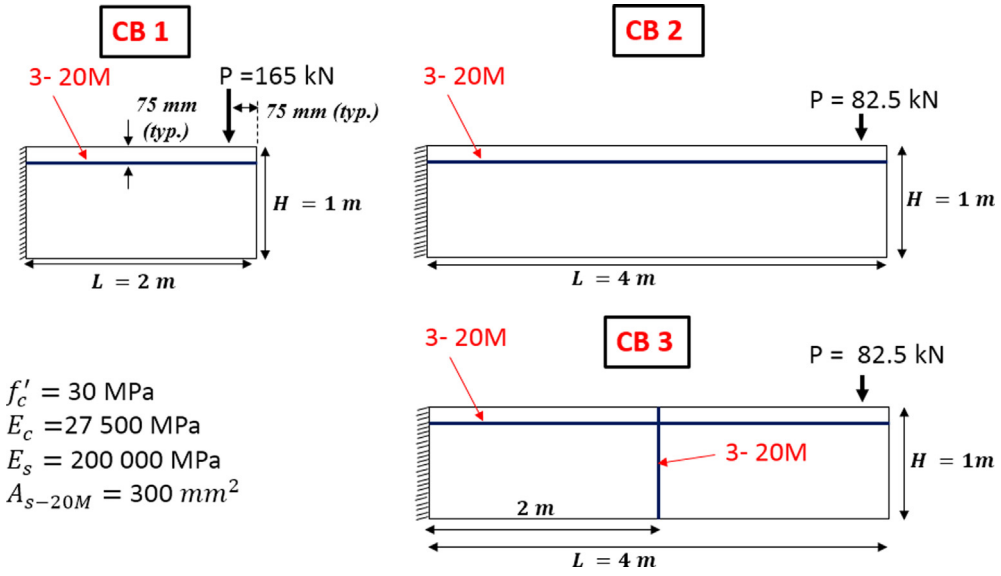

Fig. 12. Application 1: cantilever RC beams.

contour plot of the β parameter at the end of the strength reduction phase. The value of β is maximum near the nodal zone but is still less than 0.78. The stress in reinforcement at the critical section is shown in Fig. 13c for different meshes. As anticipated, all the stresses converge to the same 400 MPa value at the end of the reduction phase but with different *velocities*.

Fig. 14 shows the results for the beam CB2. As anticipated, failure occurs in the model before the end of the strength reduction phase. Principal stresses are shown in Fig. 14a at an instant just before the failure in the nodal zone. The parameter β reaches high critical values at the elements just underneath the reinforcement bed (Fig. 14b) leading to crushing of concrete. A mechanism similar to sliding failure occurs along this plane and is due to the low inclination of the compressive principal stresses with respect to the line of reinforcement (Fig. 14c).

Fig. 15 presents the results for CB3. It is interesting to see that, at the end of the strength reduction phase, the strut and nodal zones (1, 2 and 3) are clearly defined based on the results of the principal compressive stress distribution. In Fig. 15a and c, distribution of tensile stresses along longitudinal and shear reinforcement in the model are shown (continuous lines). They compare very well to the theoretical stresses computed by S&T truss model (dotted lines).

The example CB3 can be viewed as a second iteration for the SRDM algorithm (Fig. 4), where the first iteration using configuration CB2 did not result in an acceptable design. In this case, the designer added vertical ties representative of shear reinforcement (Step 4).

5.2. Deep beam with an opening

Fig. 16 shows the example of deep beam with opening presented by Tjhin et al. in [6] (example 6). It's a statically indeterminate beam simply supported on the left and fixed in the right edge. In order to compare to Tjhin et al. S&T model, the distributed load is divided in four locations over the length of the beam as shown in Fig. 16b. The reinforcement layout found by Tjhin et al. was introduced into the model (see red-coloured lines representing ties in Fig. 16b).

The model was able to reach the end of the strength reduction phase without failure. The final distribution of principal compressive stresses

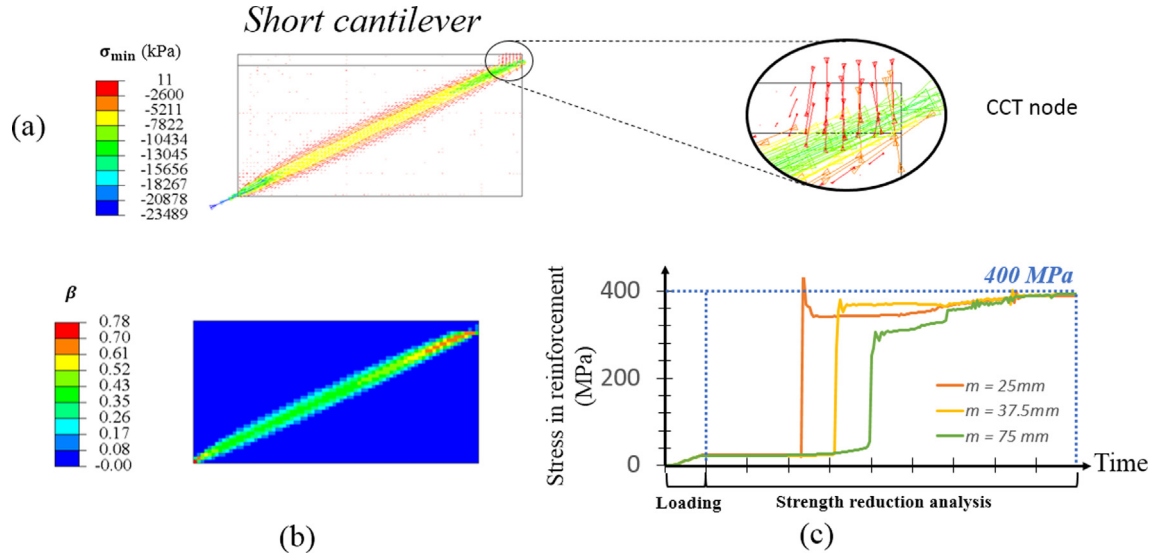

Fig. 13. Results for CB1 at the end of strength reduction phase: (a) Principal compressive stresses; (b) Distribution of β parameter and (c) Development of tensile reinforcement stresses at the critical section for different mesh sizes.

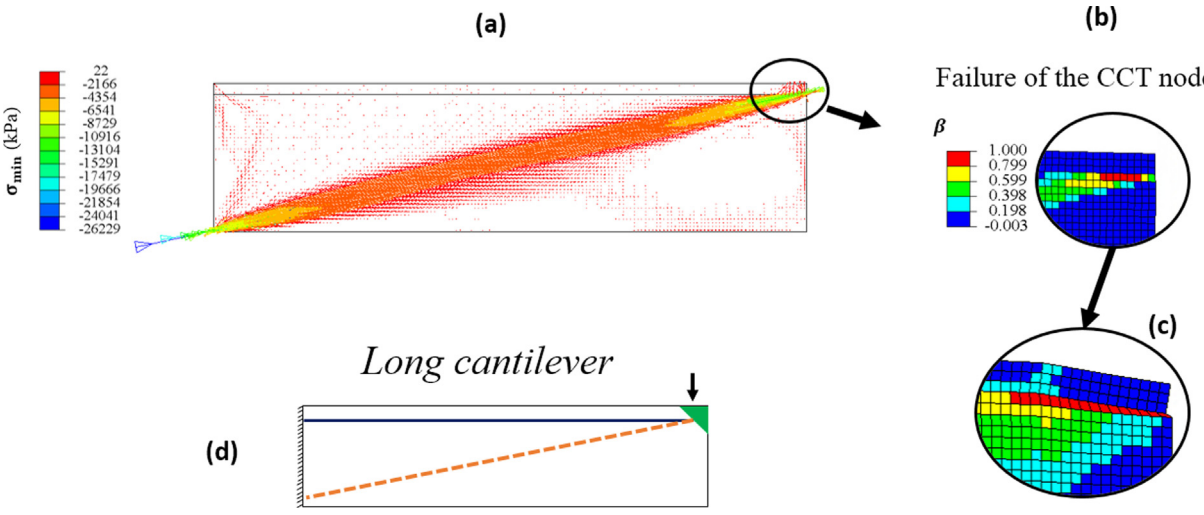

Fig. 14. Results for CB2 just before failure: (a) Principal compressive stresses; (b) Distribution of β parameter; (c) Observed sliding failure mechanism and (d) S&T model.

is shown in Fig. 16b and compares very well to the S&T model shown in Fig. 16a. The analysis exhibits approximately the same location of the struts and the nodal zones as in [6]. Comparison of the tensile forces in ties between the S&T model and the SRDM is shown in Fig. 17a. For the case of SRDM, and due to the presence of distributed struts, the tensile forces are not uniform within a tie. Therefore, the value reported in Fig. 17 for the SRDM correspond to the maximum tensile force along the tie's length.

There is in general a good agreement between the two methods when the tie is not crossed by distributed struts, e.g. HI, GH and OJ. In the cases where the ties are crossed by bottle-shaped strut, e.g. LM, AH, EO, the forces obtained by the SRDM are smaller.

Fig. 17b shows the distribution of the parameter β for two different meshes. A similar pattern is seen with a maximum value of 0.85 near the nodal zone B.

Parametric studies using the SRDM by removing some vertical ties have shown in general an ability of the model to redistribute the stresses, an ability which is higher than in the case of S&T method. This is mainly due to the fact that the model allows a continuum distribution of the flow of compressive stresses, which also has the effect to lower the demand on the reinforcement ties.

To test the mesh sensitivity with respect to the node failure mode, two analyses with two mesh sizes of 100 mm and 200 mm were conducted on a modified model without the vertical ties: CM, MQ, DN and EO. The results are shown in Fig. 18. Both models exhibit a failure before the end of the strength reduction phase, a similar distribution of the β parameter (Fig. 18a) and a similar failure mechanism as shown in Fig. 18b.

Using the SRDM method, it is not necessary to discretise the uniform load pattern into different punctual loads as it is the case for the S&T model (e.g. Fig. 16). In fact, uniform load (or any type of load) can be applied directly on the FE model, and the redistribution of this load is automatically done, for the given geometry of concrete and chosen layout of reinforcement. Fig. 19 shows the flow of compressive stresses in concrete at the end of the strength reduction phase on the same beam model but with an application of uniform loads on top of the beam. It is interesting to note that the flow is very similar to the one obtained with punctual loads (Fig. 16b). This constitutes another important advantage

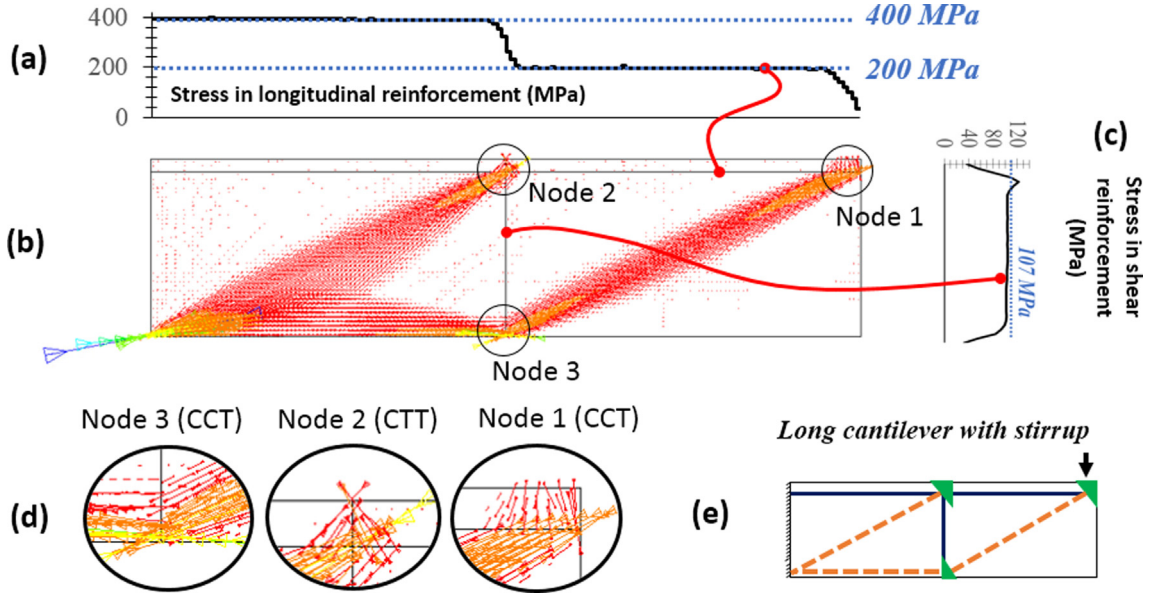

Fig. 15. Results for CB3 at the end of strength reduction phase: (a) Stresses along longitudinal reinforcement; (b) Principal compressive stresses; (c) Stresses along shear reinforcement; (d) zoom into nodal zones and (e) S&T model.

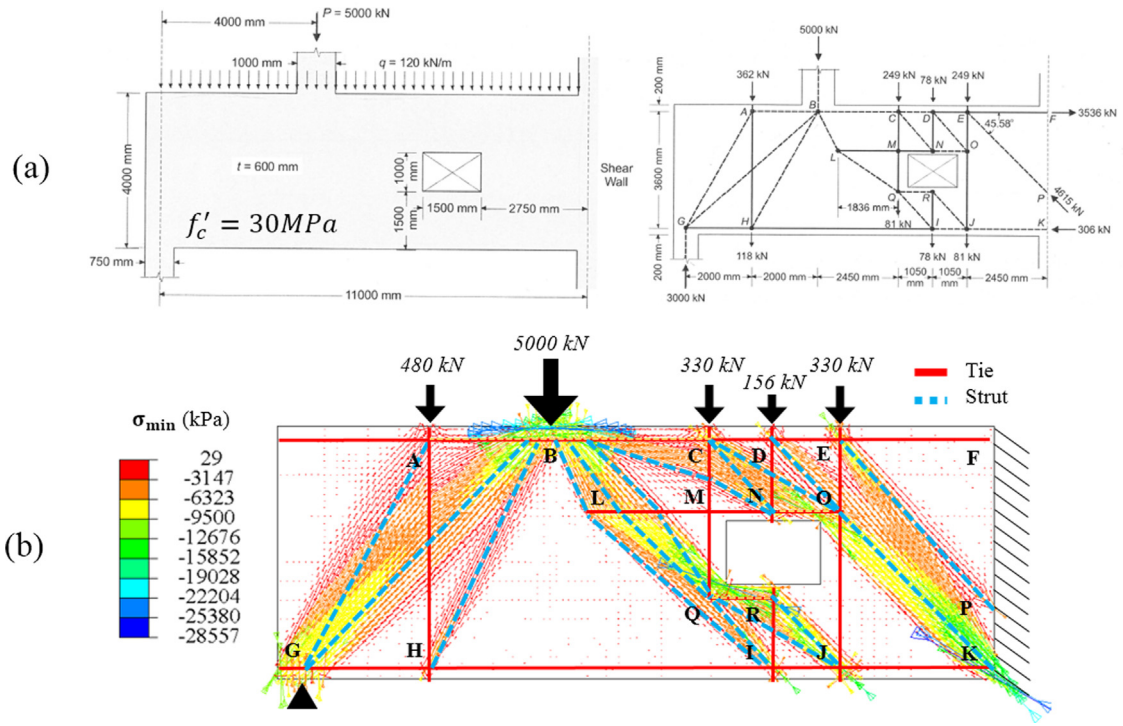

Fig. 16. Deep beam example with an opening: (a) Dimensions, loading conditions and identified S&T model (modified from [6] (b) Identification of struts and ties at the end of strength reduction phase.

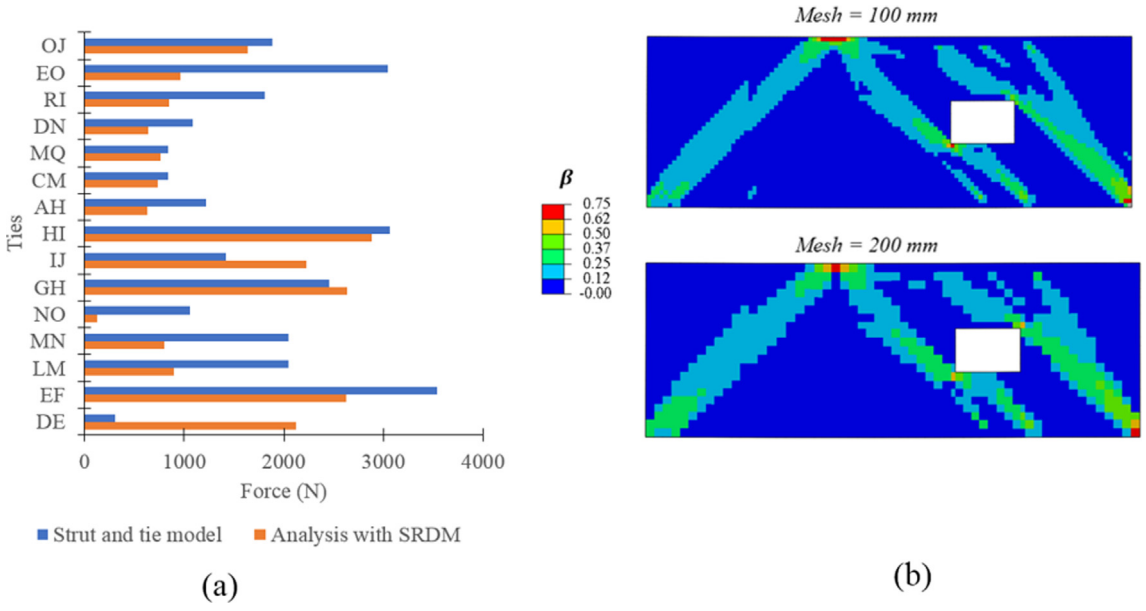

Fig. 17. Results of the SRDM: (a) Comparison of tensile forces in the ties: S&T model and SRDM and (b) Mesh sensitivity study on the β parameter.

of the SRDM and confirm.

6. Conclusions

This paper presents a new design approach of reinforced concrete structures based on the strength reduction philosophy. The developed SRDM method (Strength Reduction Design Method) is an intermediate approach between the conservative and universally well accepted strut-and-tie method and the powerful nonlinear finite element method. Using the framework of explicit quasi-static finite elements and a simple constitutive law, the structure is loaded in a first linear elastic step and then gradual isotropic degradation of the tensile strength is performed in a second step. During the fictitious degradation process, a re-organisation of the internal stresses occurs, and at the end of this step, the demand on the initially introduced layout of reinforcement can be assessed. Taking the S&T method as the reference lower bound method, the simple constitutive law can simulates the three main failure mechanisms of the struts/nodal zones in concrete (in design mode) and the ties in reinforcement (in assessment mode).

Two application examples were considered to verify and validate the proposed SRDM method. A fixed end reinforced concrete beam with different configurations and a deep beam example with opening, considered in previous studies.

The following conclusions were drawn while developing and

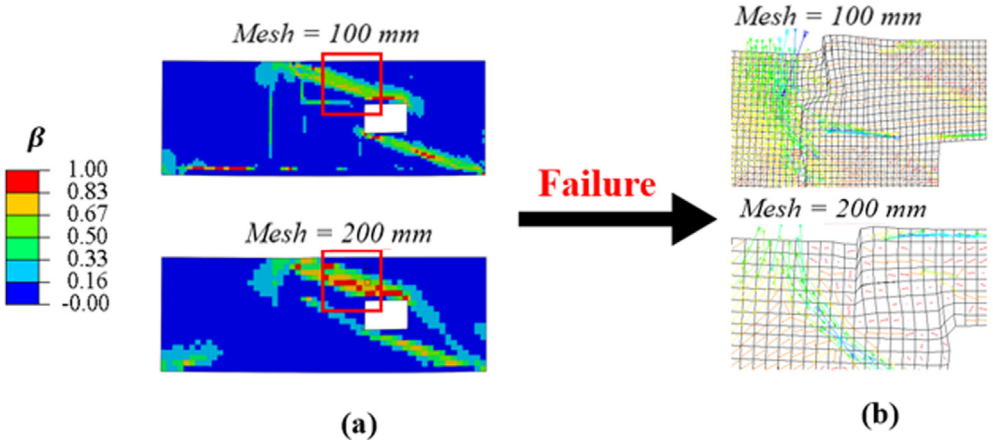

Fig. 18. Mesh sensitivity study in the case of a modified geometry of the ties: (a) Distribution of the β parameter just before failure; (b) Failure mechanism.

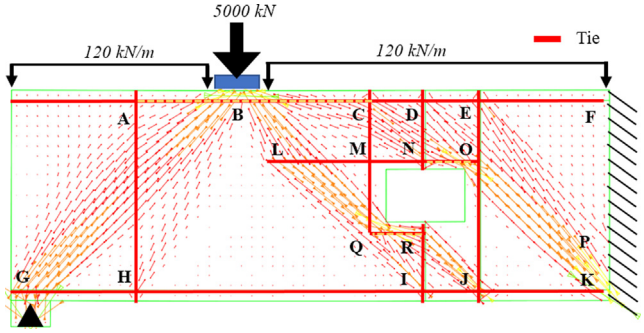

Fig. 19. Deep beam example in case of distributed loads applied on top.

applying the proposed method:

1. The SRDM method is very convenient for designing complex reinforced concrete structures. It can be used by practitioner engineers within an automatic/semi-automatic design process.
2. Contrary to non-linear finite element method which requires generally several input parameters, the SRDM requires mainly two parameters: the compressive strength of the concrete and the yield tensile strength of the reinforcement, the only two input parameters required for the conventional design practice;
3. If compared to the S&T method, the SRDM gives similar results but without the rigid-plastic assumption considered as a limitation for the S&T method. Furthermore, it is much easier to apply, especially for the case of the complex geometries;
4. Using a modified version of the MCFT, the simple developed constitutive law is quasi-mesh insensitive. The demand on the reinforcement and the failure mode related to nodal zone do not depend on the mesh refinement;

Following this research work, some further developments are underway:

1. Even if the constitutive law is developed for the general 3D state of stresses, only plane stress 2D verification and validation problems are considered in this study. SRDM is expected to allow designing complex 3D structures with complex patterns of loads whether mechanical or induced by deformation. Multiple benchmark examples are therefore being selected for the purpose of validation of the method and the extension of its applicability;
2. The generalized isotropic strength degradation scenario used in this work is more suitable for the context of designing new RC structures. For the context of assessment of existing ones, it is interesting to consider the effect of existing discrete cracks (e.g. originating from temperature gradients) on the final configuration of the flow of stresses.
3. For the SRDM to be used in a design code or standard, a reliability framework has to be developed and must be consistent with the current safety margins implicitly provided by the existing conventional design approaches.

Acknowledgements

The financial support provided by the Natural Science and Engineering Research Council of Canada is acknowledged.

References

[1] Bairan JM. Automatic generation of Strut and Tie schemes adjusted for constructability. Hormigón y Acero No 264, 3rd Trimester; 2012:67–79.
[2] Bazant ZP, Oh BH. Crack Band theory for fracture of concrete. Mater Struct 1983;16:155–77.
[3] Bendsøe MP, Kikuchi N. Generating optimal topologies in structural design using a homogenization method. Comput Methods Appl Mech Eng 1988;71:197–224.
[4] Ben Ftima M. Utilisation de la méthode des éléments finis non-linéaires pour la conception des structures en béton armé: application aux structures massives PhD thesis Canada: École Polytechnique de Montréal; 2013.
[5] Drucker DC, Greenberg HJ, Prager W. Extended limit design theorems for continuous media. Q. Appl Math 1952;9:381–9.
[6] Fédération Internationale du béton (FIB). Design examples for strut and tie models. Technical Report, CEB-FIB bulletin 61; 2011.
[7] Hibbitt HD, Karlson BI, Sorensen EP. ABAQUS version 6.14, Finite element program. Providence, R.I., USA: Hibbitt, Karlson and Sorensen; 2014.
[8] Johansen KW. Yield line theory – translated from Danish. London: Cement and Concrete Association; 1962.
[9] Liang QQ, Uy B, Steven GP. Performance-based optimization for strut-tie modeling of structural concrete. ASCE J Struct Eng 2002;128(6):815–23.
[10] Muttoni A, Schwartz J, Thürlimann B. Design of concrete structures with stress fields. Birkhäuser Verlag; 1997.
[11] Nielsen MP, Hoang LC. Limit analysis and concrete plasticity. 3rd ed. CRC Press, Taylor & Francis Group; 2011.
[12] Prior A. Applications of implicit and explicit finite element techniques to metal forming. J Mater Process Technol 1994;45(4):649–56.
[13] Querin OM, Young V, Steven GP, Xie YM. Computational efficiency and validation of bi-directional evolutionary structural optimisation. Comput Methods Appl Mech Eng 2000;189:559–73.
[14] Ruiz F, Muttoni A. On development of suitable stress fields for structural concrete. ACI Struct J 2007;104:495–502.
[15] Schlaich J, Schafer K, Jennewein M. Toward a consistent design of structural concrete. J Prestressed Concr Inst 1987;32(3):74–150.
[16] Tjhin TN, Kuchma DA. Integrated analysis and design tool for the strut and tie method. J Eng Struct 2007;29:3042–52.
[17] Tschchnigg F, Schweiger HF, Sloan SW. Slope stability analysis by means of finite element limit analysis and finite element strength reduction techniques, Part I: numerical studies considering non-associated plasticity. Comput Geotech 2015;70:169–77.
[18] Vecchio FJ, Collins MP. Modified compression field theory for reinforced concrete elements subjected to shear. ACI J 1986;83(2):219–31.
[19] Vulliet V, Ben Ftima M, Léger P. Stability of cracked concrete hydraulic structures by nonlinear quasi-static explicit finite element and 3D limit equilibrium methods. Comput Struct 2017;184:25–35.
[20] Xie YM, Steven GP. A simple evolutionary procedure for structural optimization. Comput Struct 1993;49(5):885–96.
[21] Zienkiewicz OC, Humpheson C, Lewis RW. Associated and non-associated visco-plasticity and plasticity in soil mechanics. Géotechnique 1975;25(4):671–89.